Diffusive instabilities in hyperbolic reaction-diffusion equations

Evgeny P. Zemskov[1,*] and Werner Horsthemke[2,†]
[1]*Department of Continuum Mechanics, Dorodnicyn Computing Centre, Russian Academy of Sciences, Vavilova 40, 119333 Moscow, Russia*
[2]*Department of Chemistry, Southern Methodist University, Dallas, Texas 75275-0314, USA*
(Received 8 December 2015; published 10 March 2016)

We investigate two-variable reaction-diffusion systems of the hyperbolic type. A linear stability analysis is performed, and the conditions for diffusion-driven instabilities are derived. Two basic types of eigenvalues, real and complex, are described. Dispersion curves for both types of eigenvalues are plotted and their behavior is analyzed. The real case is related to the Turing instability, and the complex one corresponds to the wave instability. We emphasize the interesting feature that the wave instability in the hyperbolic equations occurs in two-variable systems, whereas in the parabolic case one needs three reaction-diffusion equations.

DOI: 10.1103/PhysRevE.93.032211

I. INTRODUCTION

Spatiotemporal patterns and waves arise in many nonequilibrium systems at the onset of an instability of the steady state [1]. Often these systems can be modeled by standard reaction-diffusion equations. It is well known that such reaction-diffusion systems can display diffusion-driven instabilities [1]. The best-known diffusive instability is the Turing bifurcation leading to stationary spatial patterns [2]. In that same publication, Turing also described an oscillatory instability with finite wavelength. This instability, which gives rise to patterns that are periodic in both time and space, is variously known as the oscillatory Turing instability or the wave instability. It has attracted far less attention than the stationary Turing instability, though experimental observations of wave phenomena in the Belousov-Zhabotinsky (BZ) reaction dispersed in aerosol OT (AOT) water-in-oil microemulsions have led to several theoretical studies in the past two decades [3–7]. The Turing instability requires at least two species, an activator and an inhibitor, and the latter must diffuse sufficiently faster than the former. The conditions for the occurrence of a wave instability are considerably more complex. At least three species are required for reaction-diffusion systems with a diagonal diffusion matrix, i.e., no cross diffusion occurs. Typical model systems that display wave instabilities consist of an activator, an inhibitor, and a third species, coupled to the activator, whose diffusion coefficient differs significantly from the diffusion coefficients of both the activator and the inhibitor [7].

Standard reaction-diffusion equations (RDEs) are partial differential equations (PDEs) of the parabolic type [8]. In parabolic PDEs, perturbations propagate infinitely fast in the medium. It has been conjectured that certain features associated with the wave phenomena generated by the wave instability and observed in numerical simulations are caused by the infinite rate of spreading of initial perturbations due to diffusion [4]. Such an infinite rate is, however, hardly physical, and it is desirable to investigate diffusion-driven instabilities in more realistic models. Various types of hyperbolic reaction-transport equations provide a means to describe transport with inertia and to address this issue [9–11]. While the effect of inertia in the transport on the Turing instability has been studied previously [8,12,13], the case of the wave instability remains largely unexplored.

We study here the simplest type of hyperbolic reaction-transport systems, namely the so-called hyperbolic reaction-diffusion equations (HRDEs) [14–19]. We find that the wave instability in HRDEs with diagonal diffusion matrices requires only two species. The paper is organized as follows. In Sec. II we carry out a linear stability analysis of the uniform steady state to determine the conditions for diffusion-driven instabilities in two-variable HRDEs. In Sec. III we apply our results to two widely used model systems of pattern formation, namely the Brusselator and the Gierer-Meinhardt model. We discuss our results in Sec. IV.

II. LINEAR STABILITY ANALYSIS

A two-variable hyperbolic reaction-diffusion system is described by

$$\tau_u \frac{\partial^2 u}{\partial t^2} + \frac{\partial u}{\partial t} = f(u,v) + D_u \frac{\partial^2 u}{\partial x^2}, \tag{2.1a}$$

$$\tau_v \frac{\partial^2 v}{\partial t^2} + \frac{\partial v}{\partial t} = g(u,v) + D_v \frac{\partial^2 v}{\partial x^2}, \tag{2.1b}$$

where the positive constants $\tau_{u,v}$ are inertial times and $D_{u,v}$ are diffusion coefficients. Equations of this type are also employed in other contexts, such as nonlinear waves, nucleation theory, and phase-field models of phase transitions, where they are known as damped nonlinear Klein-Gordon equations; see, for example, Refs. [20–22]. We assume that the system Eq. (2.1) has a uniform steady state (USS), (u_0, v_0), given by $f(u_0, v_0) = g(u_0, v_0) = 0$. To determine the stability of the USS against spatially nonuniform perturbations, we write the densities $u = u(x,t)$ and $v = v(x,t)$ as

$$u(x,t) = u_0 + \Delta u(x,t), \tag{2.2a}$$

$$v(x,t) = v_0 + \Delta v(x,t). \tag{2.2b}$$

The perturbations $\Delta u(x,t)$ and $\Delta v(x,t)$ depend both on space and time and have the form

$$\Delta u(x,t) = C_u \exp(\lambda t + ikx), \tag{2.3a}$$

$$\Delta v(x,t) = C_v \exp(\lambda t + ikx). \tag{2.3b}$$

*zemskov@ccas.ru
†whorsthe@mail.smu.edu

Here C_u and C_v are some constants, λ is the eigenvalue, k is the wavenumber, and $i^2 = -1$. Substituting Eq. (2.2) into the evolution Eqs. (2.1) and linearizing, we find

$$\tau_u \frac{\partial^2 \Delta u}{\partial t^2} + \frac{\partial \Delta u}{\partial t} = J_{11}\Delta u + J_{12}\Delta v + D_u \frac{\partial^2 \Delta u}{\partial x^2}, \quad (2.4a)$$

$$\tau_v \frac{\partial^2 \Delta v}{\partial t^2} + \frac{\partial \Delta v}{\partial t} = J_{21}\Delta u + J_{22}\Delta v + D_v \frac{\partial^2 \Delta v}{\partial x^2}. \quad (2.4b)$$

Here J_{mn}, with $m, n = 1, 2$, are the elements of the Jacobian matrix. Exploiting the specific form Eq. (2.3), we obtain the matrix equation

$$\begin{pmatrix} J_{11} - k^2 D_u - \gamma_u & J_{12} \\ J_{21} & J_{22} - k^2 D_v - \gamma_v \end{pmatrix} \begin{pmatrix} C_u \\ C_v \end{pmatrix} = 0, \quad (2.5)$$

where we have defined

$$\gamma_{u,v} \equiv \tau_{u,v}\lambda^2 + \lambda. \quad (2.6)$$

The matrix equation has a nontrivial solution only if the determinant of the matrix is equal to zero, i.e.,

$$\gamma_u \gamma_v - \alpha\gamma_v - \beta\gamma_u + \alpha\beta - J_{12}J_{21} = 0, \quad (2.7)$$

with

$$\alpha \equiv J_{11} - k^2 D_u, \quad \beta \equiv J_{22} - k^2 D_v. \quad (2.8)$$

Equation (2.7) is a quartic equation in λ, and the form of its roots is rather complicated. Therefore, we consider the special case with $\tau_u = \tau_v \equiv \tau$, which suffices to establish the existence of the diffusion-driven Turing and wave instabilities in two-variable HRDEs. In this case Eq. (2.7) reduces to a biquadratic equation,

$$\gamma^2 - (\alpha + \beta)\gamma + \alpha\beta - J_{12}J_{21} = 0, \quad (2.9)$$

where

$$\gamma \equiv \tau\lambda^2 + \lambda. \quad (2.10)$$

The roots are given by

$$\gamma_{1,2} = \frac{\alpha + \beta}{2} \pm \sqrt{\left(\frac{\alpha + \beta}{2}\right)^2 - \alpha\beta + J_{12}J_{21}}, \quad (2.11)$$

leading to the following expressions for the four eigenvalues λ that govern the stability of the USS,

$$\lambda_{1,2} = -\frac{1}{2\tau} \pm \sqrt{\frac{1}{4\tau^2} + \frac{\gamma_1}{\tau}}, \quad (2.12a)$$

$$\lambda_{3,4} = -\frac{1}{2\tau} \pm \sqrt{\frac{1}{4\tau^2} + \frac{\gamma_2}{\tau}}. \quad (2.12b)$$

We use these expressions in the following to explore the features of diffusive instabilities in HRDEs.

A. Turing instability

A diffusion-driven instability occurs, if the USS is stable against uniform perturbations, with $k = 0$, but not against nonuniform perturbations, with $k \neq 0$. To provide a complete picture of diffusive instabilities in HRDEs, we first review the case of real λ_n corresponding to a Turing instability. An instability occurs if a real eigenvalue passes through zero, corresponding to a stationary bifurcation. The eigenvalues are real if

$$\left(\frac{\alpha - \beta}{2}\right)^2 + J_{12}J_{21} > 0, \quad (2.13a)$$

$$\frac{1}{4\tau} + \gamma > 0. \quad (2.13b)$$

Stability against uniform perturbations requires that all eigenvalues $\lambda_n(k^2 = 0), n = 1, \ldots, 4$ must have negative real parts, $\mathrm{Re}(\lambda_n) < 0$. It follows from (2.12) that this requires $\gamma_{1,2}(k^2 = 0) < 0$. This simply reflects the fact that if a real eigenvalue λ crosses zero, then γ must also cross zero; see Eq. (2.10). Taking into account Eqs. (2.11) and (2.8) we find that the condition $\gamma_{1,2}(k^2 = 0) < 0$ is fulfilled if

$$T \equiv \mathrm{tr}J = J_{11} + J_{22} < 0, \quad (2.14a)$$

$$\Delta \equiv \det J = J_{11}J_{22} - J_{12}J_{21} > 0. \quad (2.14b)$$

A real value crosses zero, if the determinant of the Jacobian crosses zero. Condition Eqs. (2.14) coincide with the well-known stability conditions for standard (parabolic) reaction-diffusion systems [8]. We note that the results for standard RDEs can be obtained using the formal substitution $\gamma \to \lambda$ in Eq. (2.9), which corresponds to the parabolic limit of the inertial time going to zero, $\tau \to 0$.

The steady state is unstable against nonuniform perturbations, i.e., a stationary diffusive instability occurs, if there exists at least one λ_n with $\mathrm{Re}(\lambda_n) > 0$ at $k^2 \neq 0$. The first inequality Eq. (2.13a) restricts the interval of the wave-number values and the second one, Eq. (2.13b), determines the allowed values of the inertial time τ. If we plot the dispersion curves, i.e., the eigenvalues λ as a function of k, at a fixed inertial time τ, then the larger τ is, the narrower is the interval of allowed values of k. Since $T < 0$ and $D_{u,v} > 0$ we have $\alpha + \beta < 0$ and $\gamma_2(k^2 \neq 0) < 0$, i.e., the eigenvalues $\lambda_{3,4}$ are always negative. The instability can occur only if $\gamma_1(k^2 \neq 0)$ changes sign. Then the eigenvalue λ_1 also changes sign, whereas λ_2 remains negative. The onset of the diffusion-driven instability corresponds to $\lambda_n = 0$ and $d\lambda_n/dk = 0$. These two equations determine the critical values of the control parameter and the critical wave number and yield

$$(J_{11} - k^2 D_u)(J_{22} - k^2 D_v) - J_{12}J_{21} = 0, \quad (2.15a)$$

$$\frac{d}{dk}[(J_{11} - k^2 D_u)(J_{22} - k^2 D_v)] = 0, \quad (2.15b)$$

i.e., the same conditions as those for the Turing bifurcation in standard parabolic RDEs. Indeed, from $\lambda = 0$ and $d\lambda/dk = 0$ it follows that $\gamma = 0$ and $d\gamma/dk = 0$; see Eq. (2.10). As expected, we find that stationary bifurcations are not affected by inertia in the transport; the instability conditions are identical for HRDEs and standard RDEs.

It is well known that a Turing bifurcation in standard RDEs requires activator-inhibitor kinetics, $J_{11} > 0$ and $J_{22} < 0$, and that the inhibitor needs to diffuse sufficiently faster than the activator, $D_v/D_u \geqslant \theta_T > 1$, where θ_T is the minimum ratio of the diffusion coefficients of inhibitor and activator needed for the occurrence of a Turing instability [8,23]. Equations (2.15) imply that the USS of HRDEs undergoes a Turing instability

for parameter values such that

$$D_v J_{11} + D_u J_{22} = \sqrt{4 D_u D_v \Delta}. \tag{2.16}$$

The critical wave number is given by

$$k_{\mathrm{T}} = \sqrt[4]{\frac{\Delta}{D_u D_v}}, \tag{2.17}$$

provided that the determinant Δ is indeed positive.

B. Wave instability

Next we deal with the case of complex λ_n. The eigenvalues have imaginary parts if either one of the inequality Eqs. (2.13) is violated, i.e.,

$$\left(\frac{\alpha-\beta}{2}\right)^2 + J_{12}J_{21} < 0, \tag{2.18}$$

or

$$\frac{1}{4\tau} + \gamma < 0. \tag{2.19}$$

The second case, Eq. (2.19), does not lead to an instability; the real part of all eigenvalues remains negative.

Introducing the additional notations

$$c \equiv (\alpha+\beta)/2, \quad d \equiv \sqrt{-J_{12}J_{21} - (\alpha-\beta)^2/4}, \tag{2.20}$$

we can write the eigenvalues in the case of Eq. (2.18) as

$$\lambda_{1,2} = -\frac{1}{2\tau} \pm \sqrt{\frac{1}{4\tau^2} + \frac{c+id}{\tau}} = -\frac{1}{2\tau} \pm y \pm iz, \tag{2.21a}$$

$$\lambda_{3,4} = -\frac{1}{2\tau} \pm \sqrt{\frac{1}{4\tau^2} + \frac{c-id}{\tau}} = -\frac{1}{2\tau} \pm y \mp iz, \tag{2.21b}$$

where

$$y = \sqrt{\frac{1}{2}\left(\sqrt{c_\tau^2 + d_\tau^2} + c_\tau\right)}, \tag{2.22a}$$

$$z = \sqrt{\frac{1}{2}\left(\sqrt{c_\tau^2 + d_\tau^2} - c_\tau\right)}, \tag{2.22b}$$

and

$$c_\tau \equiv 1/(4\tau^2) + c/\tau, \quad d_\tau \equiv d/\tau. \tag{2.23}$$

The real part of the eigenvalues is given by $\mathrm{Re}(\lambda_n) = -1/(2\tau) \pm y$ and the imaginary part by $\mathrm{Im}(\lambda_n) = \pm z$. The sign of the real part can change only for the eigenvalues $\lambda_{1,3} = -1/(2\tau) + y \pm iz$. The onset of the diffusion-driven wave instability corresponds to $\mathrm{Re}(\lambda_n) = 0$, with $k \neq 0$, and $d\mathrm{Re}(\lambda_n)/dk = 0$, i.e., $y = 1/(2\tau)$ and $dy/dk = 0$, while $\mathrm{Re}(\lambda_n) < 0$ for $k = 0$.

The boundary between the real and complex eigenvalues is described by the equation

$$\left(\frac{\alpha-\beta}{2}\right)^2 + J_{12}J_{21} \equiv h = 0, \tag{2.24}$$

which yields

$$k^2(D_u - D_v) = J_{11} - J_{22} \pm 2\sqrt{-J_{12}J_{21}}, \tag{2.25}$$

i.e., determines the zero-value curves or null-clines in parameter space.

It is rather cumbersome to derive explicit analytical conditions for the wave instability from the expressions for the dispersion curve Eqs. (2.21). We therefore proceed in an alternative manner. First we need to determine the conditions that the USS does not undergo an oscillatory instability with $k = 0$, i.e., a Hopf bifurcation. Assume that the mode $k = 0$ has a purely imaginary eigenvalue, i.e., the system is at the Hopf bifurcation point of the USS. Let $\lambda(k=0) = i\omega_{\mathrm{H}}$, with $\omega_{\mathrm{H}} \in \mathbb{R}^+$. Then $\gamma = -\tau\omega_{\mathrm{H}}^2 + i\omega_{\mathrm{H}}$, and Eq. (2.9) for $k = 0$ reads

$$\tau^2\omega_{\mathrm{H}}^4 - 2i\tau\omega_{\mathrm{H}}^3 + (\tau T - 1)\omega_{\mathrm{H}}^2 - iT\omega_{\mathrm{H}} + \Delta = 0. \tag{2.26}$$

The imaginary part vanishes when

$$\omega_{\mathrm{H}}^2 = -\frac{T}{2\tau}, \tag{2.27}$$

which requires that $T \leqslant 0$. Substituting Eq. (2.27) into the real part of Eq. (2.26), we find

$$T^2 - \frac{2}{\tau}T - 4\Delta = 0, \tag{2.28}$$

whose acceptable root is given by

$$T_{\mathrm{H}} = \frac{1}{\tau}(1 - \sqrt{1 + 4\tau^2\Delta}). \tag{2.29}$$

For small inertial times τ, we have

$$T_H = -2\Delta\tau + 2\Delta^2\tau^3 + O(\tau^5), \tag{2.30}$$

and

$$\omega_{\mathrm{H}}^2 = \Delta - \Delta^2\tau^2 + O(\tau^4). \tag{2.31}$$

In other words, the Hopf condition and the frequency of the Hopf bifurcation approach, as expected, the values of standard parabolic RDEs, namely $T_{\mathrm{H}}^* = 0$ and $\omega_{\mathrm{H}}^* = \sqrt{\Delta}$, as the inertial time goes to zero $\tau \to 0$, i.e., in the parabolic limit. As discussed above, inertia in the transport does not affect stationary bifurcation, but it advances the Hopf bifurcation point. For large inertial times, $\tau \to \infty$, the Hopf condition and the frequency of the Hopf bifurcation approach $T_{\mathrm{H}} \to -2\sqrt{\Delta}$ and $\omega_{\mathrm{H}} \to 0$.

Combining condition Eqs. (2.14), which ensure that the USS cannot undergo a stationary bifurcation with $k = 0$, with the condition $T < T_{\mathrm{H}}$, which ensures that the USS cannot undergo a Hopf bifurcation with $k = 0$, we find that the standard stability conditions for parabolic RDEs Eqs. (2.14) need to be replaced by the stability conditions

$$T < T_{\mathrm{H}}, \tag{2.32a}$$

$$\Delta > 0, \tag{2.32b}$$

for HRDEs.

The wave instability occurs when the real part of an eigenvalue with $k \neq 0$ vanishes. To obtain the conditions for this instability, we proceed in a similar manner, now with $k \neq 0$, i.e., $\lambda(k \neq 0) = i\omega_{\mathrm{w}}$. We find

$$\tau^2\omega_{\mathrm{w}}^4 - 2i\tau\omega_{\mathrm{w}}^3 + [(\alpha+\beta)\tau - 1]\omega_{\mathrm{w}}^2 - i(\alpha+\beta)\omega_{\mathrm{w}} + \alpha\beta - J_{12}J_{21} = 0. \tag{2.33}$$

The imaginary part yields

$$\omega_{\rm w}^2 = -\frac{\alpha+\beta}{2\tau} = -\frac{T - k^2(D_u + D_v)}{2\tau}, \tag{2.34}$$

which requires $T \leqslant k^2(D_u + D_v)$. Substituting Eq. (2.34) into the real part of Eq. (2.33), we obtain

$$c_0 k^4 + c_2 k^2 + c_4 = 0, \tag{2.35}$$

with

$$c_0 = (D_u - D_v)^2, \tag{2.36}$$

$$c_2 = -2\left(T - \frac{1}{\tau}\right)(D_u + D_v) + 4(D_v J_{11} + D_u J_{22}), \tag{2.37}$$

$$c_4 = T^2 - \frac{2}{\tau}T - 4\Delta. \tag{2.38}$$

The coefficient c_0 is positive, and stability of the USS against uniform perturbations implies that so is the coefficient c_4; see Eq. (2.28). Since k^2 must be positive, it follows that the coefficient c_2 must be negative:

$$D_v J_{11} + D_u J_{22} < \frac{1}{2}\left(T - \frac{1}{\tau}\right)(D_u + D_v) < 0, \tag{2.39}$$

since $T < T_{\rm H} \leqslant 0$. As discussed above, for activator-inhibitor kinetics we have $J_{11} > 0$ and $J_{22} < 0$. Consequently, Eq. (2.39) will be fulfilled if the activator diffuses sufficiently fast compared to the inhibitor, $D_u/D_v \geqslant \Theta_{\rm w}$, where $\Theta_{\rm w}$ is the minimum ratio of the diffusion coefficients of activator and inhibitor needed for the occurrence of a wave instability. Note that this is opposite to the requirement for a Turing bifurcation; see Sec. II A.

The roots of Eq. (2.35) are given by

$$k_{1,2}^2 = \frac{-c_2 \pm \sqrt{c_2^2 - 4c_0 c_4}}{2c_0}. \tag{2.40}$$

A wave instability occurs when Eq. (2.35) has a degenerate or double root. The USS of a HRDE undergoes a wave instability for parameter values such that

$$c_2^2 - 4c_0 c_4 = 0, \tag{2.41}$$

and the critical wave number is given by

$$k_{\rm w} = \sqrt{-\frac{c_2}{2c_0}}, \tag{2.42}$$

provided that indeed c_2 is negative.

III. MODEL SYSTEMS

We apply our results from the linear stability analysis to two iconic models of pattern formation, namely the Brusselator [24] and the Gierer-Meinhardt model [25]. The first is a cross activator-inhibitor system and the second a pure activator-inhibitor system. These models, and variants thereof, have been widely used to elucidate various aspects of diffusive instabilities in reaction-diffusion systems; see, for example, Refs. [4,26–39].

A. Brusselator

The HRDEs for the Brusselator are given by

$$\tau\frac{\partial^2 u}{\partial t^2} + \frac{\partial u}{\partial t} = A - (B+1)u + u^2 v + D_u\frac{\partial^2 u}{\partial x^2}, \tag{3.1a}$$

$$\tau\frac{\partial^2 v}{\partial t^2} + \frac{\partial v}{\partial t} = Bu - u^2 v + D_v\frac{\partial^2 v}{\partial x^2}, \tag{3.1b}$$

where A and B are positive constants. The Brusselator has a unique USS $(A, B/A)$ with the Jacobian matrix

$$J = \begin{pmatrix} B-1 & A^2 \\ -B & -A^2 \end{pmatrix}. \tag{3.2}$$

The standard stability condition Eqs. (2.14) are satisfied as follows: the trace $T = B - 1 - A^2$ is negative for $B < 1 + A^2 \equiv B_{\rm H}^*$, whereas the determinant $\Delta = A^2$ is always positive. Equation (2.29) implies that the USS undergoes a Hopf bifurcation, with $k_{\rm H} = 0$, as the control parameter B increases, at

$$B_{\rm H} = 1 + A^2 + \frac{1}{\tau}(1 - \sqrt{1 + 4\tau^2 A^2}) < B_{\rm H}^*. \tag{3.3}$$

Consequently the stability condition Eqs. (2.32) are fulfilled for $B < B_{\rm H}$.

As mentioned in Sec. II A, the Turing bifurcation in a two-variable standard reaction-diffusion system requires activator-inhibitor kinetics. The Brusselator is of the cross activator-inhibitor type, because $J_{11} > 0$, $J_{22} < 0$, $J_{12} > 0$, and $J_{21} < 0$. Therefore, $J_{12}J_{21} < 0$, and the null-cline equation $h = 0$, in the form of Eq. (2.25), becomes

$$k^2(D_u - D_v) = B - 1 + A^2 \pm 2A\sqrt{B}. \tag{3.4}$$

The null-clines $h(k, B) = 0$ are shown in Fig. 1. If $D_u > D_v$, Fig. 1(a), then for any value of the control parameter B there coexist intervals of the wave number k, where the eigenvalues λ are real, $h > 0$, with those where the eigenvalues are complex, $h < 0$. In contrast, if $D_u < D_v$, Fig. 1(b), there exist intervals of B where the eigenvalues are real for the whole range of k. As discussed in Sec. II A, a Turing instability in standard (parabolic) reaction-diffusion systems can only occur if $D_u < D_v$ and the Turing conditions for HRDEs coincide with those of parabolic RDEs. Consequently, $D_u < D_v$ is a necessary condition for the Turing instability, i.e., a real eigenvalue at $k \neq 0$, passing through zero, in both HRDEs and standard RDEs.

1. *Turing instability*

The behavior of the real eigenvalue $\lambda_1 = \lambda_1(k)$ as function of the wave number at several values of the control parameter B is shown in Fig. 2. The variation of the eigenvalue λ_1 is compared with γ_1, which is the eigenvalue in the case of the standard (parabolic) Brusselator. Both eigenvalues of the hyperbolic and parabolic Brusselator systems change sign at the Turing instability point with the same critical values $B_{\rm T}$ and $k_{\rm T}$,

$$B_{\rm T} = (1 + A\sqrt{D_u/D_v})^2, \quad k_{\rm T} = \sqrt{A/\sqrt{D_u D_v}}, \tag{3.5}$$

of the control parameter and the wave number, respectively. To satisfy the condition Eqs. (2.32), the critical value for the

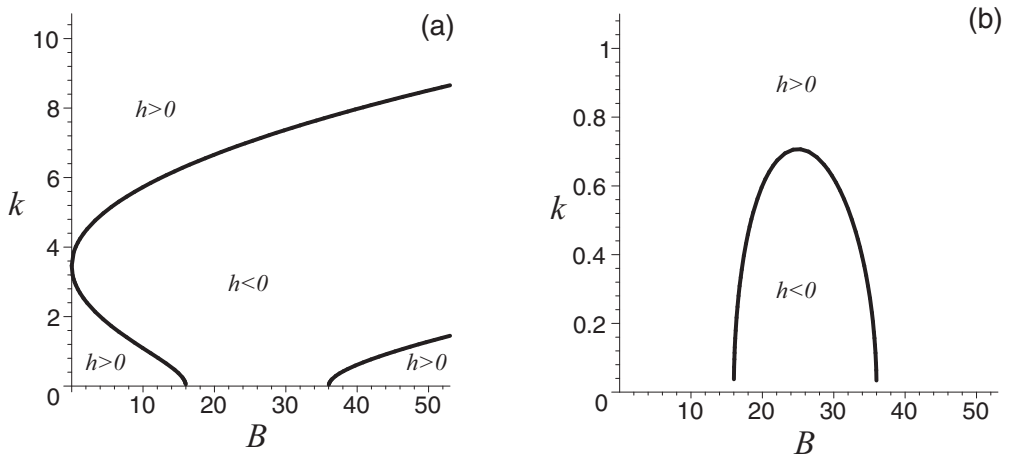

FIG. 1. Wave number versus control parameter k-B diagram for the hyperbolic Brusselator with fixed $A = 5$ and (a) $D_u = 3$, $D_v = 1$ and (b) $D_u = 1$, $D_v = 3$. The curves represent the null-cline equation $h(k, B) = 0$.

Turing instability must be less than the critical value for the Hopf instability, i.e.,

$$B_{\mathrm{T}} < B_{\mathrm{H}}, \tag{3.6}$$

which will be the case for sufficiently large values of $\theta = D_v/D_u$. Then the Turing instability occurs first in the system as B is increased. At the onset of the Turing instability, the curves $\lambda_1 = \lambda_1(k)$ and $\gamma_1 = \gamma_1(k)$ touch the k axis at the same point, as follows from Eq. (2.10).

For the parameter values $A = 5$, $D_u = 1$, $D_v = 3$, and $\tau = 1$, the Hopf condition Eq. (3.3) yields $B_{\mathrm{H}} = 16.950124$, with $\omega_{\mathrm{H}} = 2.1271901$ according to Eq. (2.27). The Turing condition Eqs. (3.5) yield $B_{\mathrm{T}} = 15.106836$ and $k_{\mathrm{T}} = 1.6990442$. As required, the critical value B_{T} is less than the critical value B_{H}; the Turing instability occurs before the Hopf bifurcation.

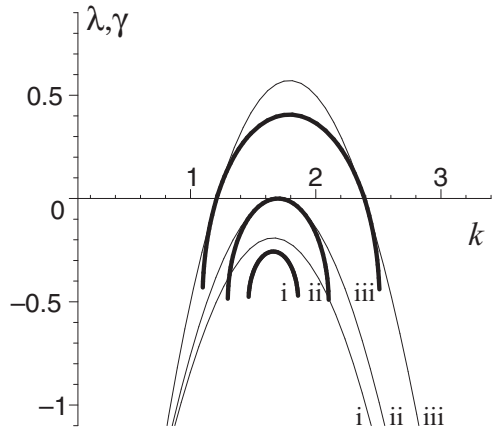

FIG. 2. Turing instability. The dispersion curves for real eigenvalues λ_1 (thick line) and γ_1 (thin line) for the hyperbolic and parabolic Brusselators, respectively, are shown for various values of the control parameter B: (i) before the Turing bifurcation point at $B = 14.6$, (ii) at the Turing bifurcation point with the critical value $B_{\mathrm{T}} = 15.106836$ and the critical wave number $k_{\mathrm{T}} = 1.6990442$, and (iii) beyond the Turing instability at $B = 16.5$. The model parameters are fixed at $A = 5$, $D_u = 1$, $D_v = 3$, i.e., the case of Fig. 1(b), and $\tau = 1$.

2. *Wave instability*

In the case of complex eigenvalues λ, the two criteria for the onset of instability are satisfied if $D_u > D_v$ as discussed above, see also Fig. 1(a). An example is presented graphically in Fig. 3. For the parameter values $A = 5$, $D_u = 3$, $D_v = 1$, and $\tau = 1$, the wave instability condition Eqs. (2.41) and (2.42) yield the critical values $B_{\mathrm{w}} = 1.4693878$ and $k_{\mathrm{w}} = 3.4255939$ of the control parameter and the wave number, respectively. The frequency of the wave instability is $\omega_{\mathrm{w}} = 5.9778503$ according to Eq. (2.34). As required, the critical value B_{w} is less than the critical value B_{H}; the wave instability occurs before the Hopf bifurcation. At large values of the inertial time, the solution is located in the vicinity of the null-cline $h = 0$.

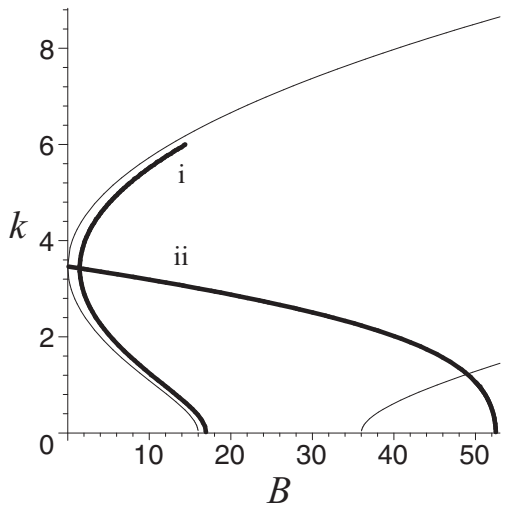

FIG. 3. Criteria for the onset of the wave instability depicted by thick lines (i) $\mathrm{Re}(\lambda_{1,3}) = -1/(2\tau) + y = 0$ and (ii) $d\mathrm{Re}(\lambda_{1,3})/dk = dy/dk = 0$ in the wave number versus control parameter k-B plane for the hyperbolic Brusselator at fixed $A = 5$, $D_u = 3$, $D_v = 1$, i.e., the case of Fig. 1(a), and $\tau = 1$. The intersection of (i) and (ii) curves corresponds to the wave bifurcation point with the critical values $B_{\mathrm{w}} = 1.4693878$ and $k_{\mathrm{w}} = 3.4255939$. The thin lines represent the null-cline equation $h = 0$; see Fig. 1(a).

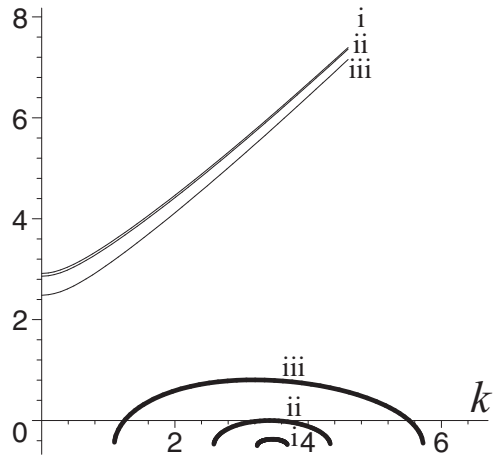

FIG. 4. Wave instability. The dispersion curves for real $\mathrm{Re}(\lambda_{1,3}) = -1/(2\tau) + y$ (thick line) and imaginary $\mathrm{Im}(\lambda_{1,3}) = z$ (thin line) parts of the eigenvalues $\lambda_{1,3}$ for the hyperbolic Brusselator at various values of the control parameter B: (i) below the wave bifurcation point at $B = 0.1$, (ii) at the bifurcation point with the critical value $B_w = 1.4693878$ and the critical wave number $k_w = 3.4255939$, and (iii) beyond the wave instability point at $B = 10$. The model parameters are fixed at $A = 5$, $D_u = 3$, $D_v = 1$, i.e., the case of Fig. 1(a), and $\tau = 1$.

As discussed above, if $D_u < D_v$, a common solution to the two instability criteria does not exist; see Fig. 1(b).

The onset of the wave instability for this example is shown in Fig. 4. The dispersion curves for the real and imaginary parts of the eigenvalue demonstrate the typical behavior for the wave instability; see, for example, Fig. 4 in Ref. [3]. The dependence of the critical values B_w and k_w on the inertial time τ shows contrasting behavior. The critical value of the control parameter decreases, whereas the critical wavenumber increases, as τ increases; see Fig. 5. When the inertial time goes to zero, the limit case of parabolic equations, the critical value of the control parameter grows without bound. Note, however,

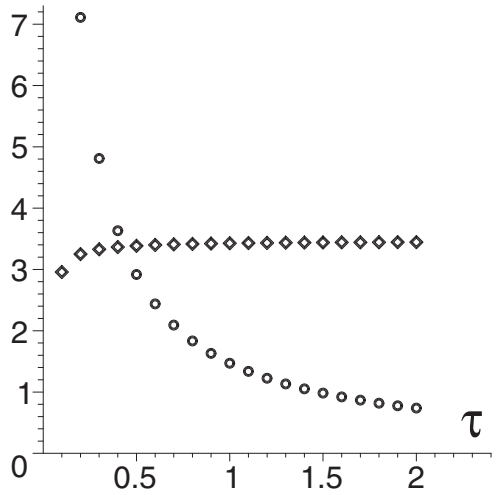

FIG. 5. Wave instability. Critical values B_w (circles) and k_w (diamonds) as functions of the inertial time τ for $A = 5$, $D_u = 3$, and $D_v = 1$, i.e., the case of Fig. 1(a), for the hyperbolic Brusselator.

that B_w must be smaller than B_H as discussed above; otherwise, the stability condition Eqs. (2.32) are not fulfilled and the USS has already become unstable and undergone a uniform Hopf bifurcation. This implies that there exists a minimum value of the inertial time τ, given by

$$B_w(\tau_{\min}) = B_H, \tag{3.7}$$

for a wave instability to occur in the hyperbolic Brusselator. For the parameter values $A = 5$, $D_u = 3$, and $D_v = 1$, the condition Eq. (3.7) yields a value of $\tau_{\min} = 0.041666667$.

B. Gierer-Meinhardt model

The HRDEs for the Gierer-Meinhardt model are given by

$$\tau\frac{\partial^2 u}{\partial t^2} + \frac{\partial u}{\partial t} = 1 - u + a\frac{u^2}{v} + D_u\frac{\partial^2 u}{\partial x^2}, \tag{3.8a}$$

$$\tau\frac{\partial^2 v}{\partial t^2} + \frac{\partial v}{\partial t} = b(u^2 - v) + D_v\frac{\partial^2 v}{\partial x^2}, \tag{3.8b}$$

where a and b are positive constants. The Gierer-Meinhardt model has a unique USS state $(1 + a, (1 + a)^2)$ with the Jacobian matrix

$$J = \begin{pmatrix} (a-1)/(a+1) & -a/(1+a)^2 \\ 2b(1+a) & -b \end{pmatrix}. \tag{3.9}$$

The stability condition Eqs. (2.14) are satisfied as follows: the trace $T = (a - 1)/(a + 1) - b$ is negative for $b > (a - 1)/(a + 1) \equiv b_H^*$ and the determinant $\Delta = b$ is always positive. Equation (2.29) implies that the USS undergoes a Hopf bifurcation, with $k_H = 0$, as the control parameter b decreases, at b_H given by

$$b_H = \frac{a-1}{a+1} - \frac{1}{\tau}(1 - \sqrt{1 + 4\tau^2 b_H}), \tag{3.10}$$

which has one acceptable root,

$$b_H = \frac{1}{\tau}\Bigg[-1 + \left(2 + \frac{a-1}{a+1}\right)\tau + \sqrt{1 - 4\tau + 4\tau^2\left(1 + \frac{a-1}{a+1}\right)}\Bigg]. \tag{3.11}$$

Consequently the stability condition Eqs. (2.32) are fulfilled for $b > b_H$.

The Gierer-Meinhardt model is of the pure activator-inhibitor type, because $J_{11} > 0$, $J_{22} < 0$, $J_{12} < 0$, and $J_{21} > 0$. We have again $J_{12}J_{21} < 0$, and the null-cline equation $h = 0$ in the form of Eq. (2.25) becomes

$$k^2(D_u - D_v) = \frac{a-1}{a+1} + b \pm 2\sqrt{\frac{2ab}{a+1}}. \tag{3.12}$$

We see that the $k - b$ dependence, $k^2 \propto b \pm \sqrt{b}$, is identical to the $k - B$ dependence, Eq. (3.4), for the Brusselator. Therefore, the diagrams in Fig. 1 apply qualitatively also to the Gierer-Meinhardt model and we do not show them here. We choose b as the control parameter for the Gierer-Meinhardt model and consider the cases of the Turing and wave bifurcations as above for the Brusselator model.

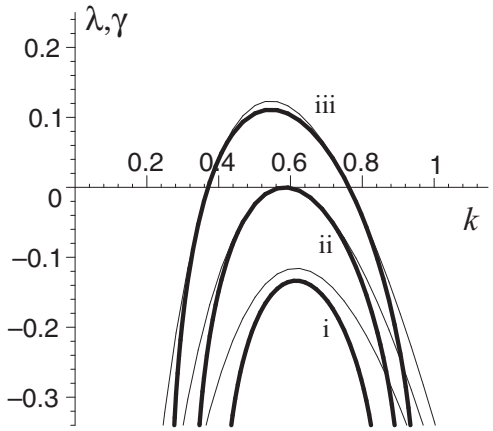

FIG. 6. Turing instability. The dispersion curves for real eigenvalues λ_1 (thick line) and γ_1 (thin line) for the hyperbolic and parabolic Gierer-Meinhardt models, respectively, at various values of the control parameter b: (i) before the Turing bifurcation point at $b = 8$, (ii) at the Turing bifurcation point with the critical value $b_{\rm T} = 5.8359213$ and the critical wave number $k_{\rm T} = 0.58450046$, and (iii) beyond the Turing bifurcation point at $b = 4$. The model parameters are fixed at $a = 9$, $D_u = 1$, $D_v = 50$, and $\tau = 1$.

1. Turing instability

At the Turing bifurcation point, the critical values $b_{\rm T}$ and $k_{\rm T}$ of the control parameter and the wave number, respectively, read

$$b_{\rm T} = \frac{D_v}{D_u}\left(-1 + \sqrt{1 + \frac{a-1}{a+1}}\right)^2, \tag{3.13a}$$

$$k_{\rm T} = \sqrt[4]{\frac{b_{\rm T}}{D_u D_v}}. \tag{3.13b}$$

To satisfy the condition Eqs. (2.32), the critical value for the Turing instability must be greater than the critical value for the Hopf instability $b_{\rm H}$, i.e.,

$$b_{\rm T} > b_{\rm H}, \tag{3.14}$$

which will be the case for sufficiently large values of $\theta = D_v/D_u$. Then the Turing instability occurs first in the system as b is decreased. The corresponding dispersion curves for λ_1 and γ_1 in the vicinity of the Turing bifurcation point are shown in Fig. 6.

For the parameter values $a = 9$, $D_u = 1$, $D_v = 50$, and $\tau = 1$, the Hopf condition Eq. (3.10) yields $b_{\rm H} = 3.8493901$, with $\omega_{\rm H} = 1.2347854$ according to Eq. (2.27). The Turing condition Eqs. (3.13) yield $b_{\rm T} = 5.8359213$ and $k_{\rm T} = 0.58450046$. As required, the critical value $b_{\rm T}$ is greater than the critical value $b_{\rm H}$; the Turing instability occurs before the Hopf bifurcation.

The behavior of the dispersion curves in the Gierer-Meinhardt model resembles the Turing case in the Brusselator illustrated in Fig. 2. The difference is that in the Gierer-Meinhardt model the Turing instability occurs as the control parameter decreases, whereas in the Brusselator the instability arises as the control parameter increases. Note also that the maxima of the dispersion curves in both models move in opposite directions: to the left in the Gierer-Meinhardt model and to the right in the Brusselator.

2. Wave instability

The diagram of the dispersion curves for the wave instability (Fig. 7) is similar to the Turing case. For the parameter values $a = 2$, $D_u = 5$, $D_v = 4$, and $\tau = 3$, the wave instability condition Eqs. (2.41) and (2.42) yield the critical values $b_{\rm w} = 5.4166667$ and $k_{\rm w} = 1.6583124$ of the control parameter and the wave number, respectively. The frequency of the wave instability is $\omega_{\rm w} = 2.2298480$ according to Eq. (2.34). The Hopf condition Eqs. (3.10) and (2.27) yield $b_{\rm H} = 4.0275875$ and $\omega_{\rm H} = 0.78467129$, respectively. As required, the critical value $b_{\rm w}$ is greater than the critical value $b_{\rm H}$; the wave instability occurs before the Hopf bifurcation.

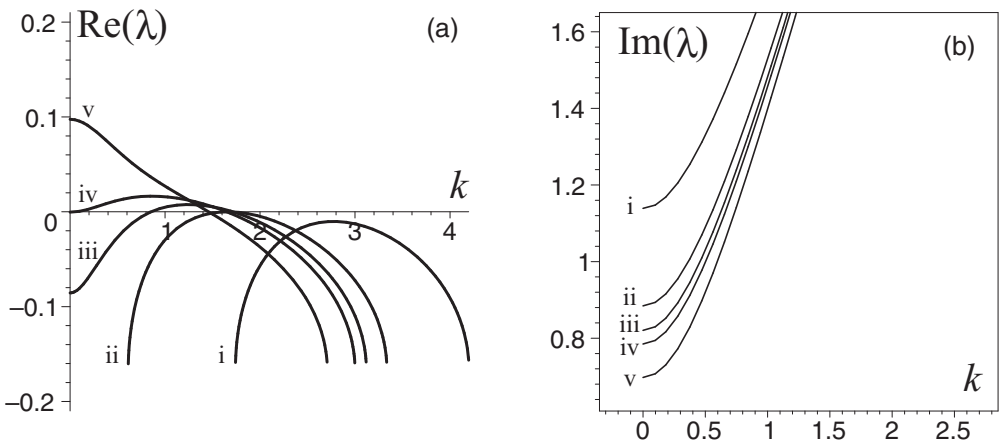

FIG. 7. Wave instability. The dispersion curves for (a) real $\mathrm{Re}(\lambda_{1,3}) = -1/(2\tau) + y$ and (b) imaginary $\mathrm{Im}(\lambda_{1,3}) = z$ parts of the eigenvalues $\lambda_{1,3}$ for the hyperbolic Gierer-Meinhardt model at various values of the control parameter b: (i) before the wave bifurcation point at $b = 10$, (ii) at the bifurcation point with the critical value $b_{\rm w} = 5.4166667$ and the critical wave number $k_{\rm w} = 1.6583124$, and beyond the wave bifurcation point at (iii) $b = 4.5$, (iv) $b = 4.03$, and (v) $b = 3$. (The critical value for the Hopf bifurcation is $b_{\rm H} = 4.0275875$.) The model parameters are fixed at $a = 2$, $D_u = 5$, $D_v = 4$, and $\tau = 3$.

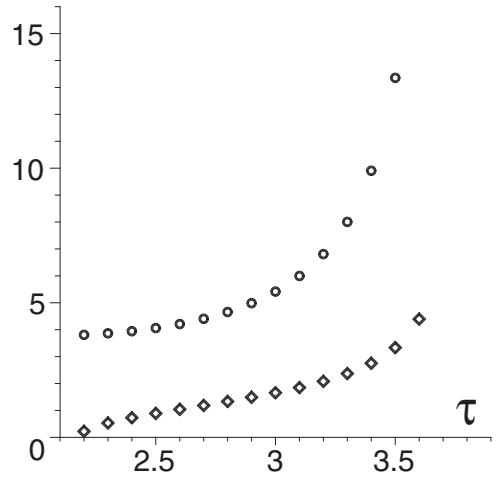

FIG. 8. Wave instability. Critical values b_w (circles) and k_w (diamonds) as functions of the inertial time τ for $a = 2$, $D_u = 5$, and $D_v = 4$ for the hyperbolic Gierer-Meinhardt model.

The dispersion curve for the real part of $\lambda_{1,3}$, Fig. 7(a), moves to the left as the control parameter decreases and the wave instability arises. In contrast to the Brusselator, the maximum shows a pronounced shift, to the left, as the control parameter is decreased through the wave instability threshold, and is eventually located at $k = 0$, curve (v) in Fig. 7(a). Note that this occurs after the Hopf bifurcation at $b_H = 4.0275875$, curve (iv) in Fig. 7(a).

The dependence of the critical values b_w and k_w for the wave bifurcation in the Gierer-Meinhardt model on the inertial time, Fig. 8, also differs from that of the Brusselator, Fig. 5. As the inertial time increases, so does the critical value b_w. Note again that there exists a minimum value of the inertial time for a wave instability to occur. For the parameter values $a = 2$, $D_u = 5$, and $D_v = 4$, the condition $b_w(\tau_{min}) = b_H$ yields a value of $\tau_{min} = 2.1776445$.

IV. CONCLUSION

We have studied hyperbolic reaction-diffusion systems and derived the criteria for diffusion-driven instabilities in such systems. We have illustrated our general results by applying them to two widely used model systems, namely the Brusselator and the Gierer-Meinhardt model.

Before discussing our findings, we want to stress that the form of the hyperbolic Eqs. (2.1) is important for the existence of diffusive instabilities. The hyperbolic systems must indeed be HRDEs, in the sense that RDEs are the parabolic limit case. In other words, the first-order derivatives with respect to time play a crucial role. As mentioned in Sec. II, HRDEs Eqs. (2.1) are known as damped nonlinear Klein-Gordon equations in other fields. The question arises if diffusive instabilities can occur in coupled Klein-Gordon equations,

$$\tau \frac{\partial^2 u}{\partial t^2} = f(u,v) + D_u \frac{\partial^2 u}{\partial x^2}, \tag{4.1a}$$

$$\tau \frac{\partial^2 v}{\partial t^2} = g(u,v) + D_v \frac{\partial^2 v}{\partial x^2}. \tag{4.1b}$$

The linear stability analysis of Eq. (4.1), see Sec. II, yields the matrix equation

$$\begin{pmatrix} J_{11} - k^2 D_u - \tau\lambda^2 & J_{12} \\ J_{21} & J_{22} - k^2 D_v - \tau\lambda^2 \end{pmatrix} \begin{pmatrix} C_u \\ C_v \end{pmatrix} = 0. \tag{4.2}$$

The corresponding eigenvalues

$$\lambda_{1,2} = \pm \frac{1}{\sqrt{\tau}} \sqrt{\frac{\alpha+\beta}{2} + \sqrt{\left(\frac{\alpha-\beta}{2}\right)^2 + J_{12}J_{21}}}, \tag{4.3a}$$

$$\lambda_{3,4} = \pm \frac{1}{\sqrt{\tau}} \sqrt{\frac{\alpha+\beta}{2} - \sqrt{\left(\frac{\alpha-\beta}{2}\right)^2 + J_{12}J_{21}}}, \tag{4.3b}$$

cannot change sign, if they are real, and no bifurcation can occur. If the eigenvalues are complex, the real part,

$$\mathrm{Re}(\lambda) = \pm \frac{1}{\sqrt{\tau}} \sqrt{\frac{1}{2}\left(\frac{\alpha+\beta}{2} + \sqrt{\alpha\beta - J_{12}J_{21}}\right)}, \tag{4.4}$$

cannot change sign, and again no bifurcation can occur.

Hyperbolic reaction-diffusion system can undergo two types of diffusive instabilities, the Turing instability and the wave instability. As far as the Turing instability is concerned, the conditions are the same as for standard reaction-diffusion equations. At least two variables are required, and the kinetics need to be of the activator-inhibitor type. Further, the inhibitor needs to diffuse sufficiently fast, compared to the activator, for a Turing bifurcation to occur in both hyperbolic and parabolic systems. The critical values for the Turing instability are independent of the inertial time and coincide with the critical values for standard parabolic reaction-diffusion systems.

As far as the wave instability is concerned, the conditions for hyperbolic and parabolic systems differ qualitatively. It is the main result of this work that the wave instability requires *only two species* in hyperbolic reaction-diffusion equations, in contrast to standard parabolic reaction-diffusion equations where at least three species are required. The critical values for the wave instability depend on the inertial time, in contrast to the case of the Turing instability. Further, the wave instability cannot occur for arbitrarily small inertial times. A minimum distance from the parabolic limit case is required. Another important difference with the Turing instability is the requirement that it is the activator that needs to diffuse sufficiently fast, compared to the inhibitor, for a wave instability to occur. This is similar to the fact that, as discussed in Sec. I, wave instabilities in standard reaction-diffusion systems typically occur in models consisting of an activator, an inhibitor, and a third species, coupled to the activator, which diffuses significantly faster than both the activator and the inhibitor.

ACKNOWLEDGMENT

The work of E.P.Z. was supported in part by the Russian Foundation for Basic Research (RFBR), Grant No. 13-01-00333-a.

[1] M. Cross and H. Greenside, *Pattern Formation and Dynamics in Nonequilibrium Systems* (Cambridge University Press, Cambridge, 2009).

[2] A. M. Turing, The chemical basis of morphogenesis, Philos. Trans. R. Soc. London B **237**, 37 (1952).

[3] A. M Zhabotinsky, M. Dolnik, and I. R. Epstein, Pattern formation arising from wave instability in a simple reaction-diffusion system, J. Chem. Phys. **103**, 10306 (1995).

[4] V. K. Vanag and I. R. Epstein, Comparative analysis of packet and trigger waves originating from a finite wavelength instability, J. Phys. Chem. A **106**, 11394 (2002).

[5] V. K. Vanag and I. R. Epstein, Diffusive instabilities in heterogeneous media, J. Chem. Phys. **119**, 7297 (2003).

[6] V. K. Vanag and I. R. Epstein, Subcritical wave instability in reaction-diffusion systems, J. Chem. Phys. **121**, 890 (2004).

[7] V. K. Vanag and I. R. Epstein, Cross-diffusion and pattern formation in reaction-diffusion systems, Phys. Chem. Chem. Phys. **11**, 897 (2009).

[8] V. Méndez, S. Fedotov, and W. Horsthemke, *Reaction-Transport Systems: Mesoscopic Foundations, Fronts, and Spatial Instabilities* (Springer, Heidelberg, 2010).

[9] V. Méndez, D. Campos, and W. Horsthemke, Growth and dispersal with inertia: Hyperbolic reaction-transport systems, Phys. Rev. E **90**, 042114 (2014).

[10] G. Abramson, A. R. Bishop, and V. M. Kenkre, Effects of transport memory and nonlinear damping in a generalized Fisher's equation, Phys. Rev. E **64**, 066615 (2001).

[11] E. P. Zemskov, M. A. Tsyganov, and W. Horsthemke, Wavy fronts in a hyperbolic FitzHugh-Nagumo system and the effects of cross diffusion, Phys. Rev. E **91**, 062917 (2015).

[12] W. Horsthemke, Spatial instabilities in reaction random walks with direction-independent kinetics, Phys. Rev. E **60**, 2651 (1999).

[13] W. Horsthemke, Pattern formation in random walks with inertia, in *Noise in Complex Systems and Stochastic Dynamics III*, Proc. of SPIE, Vol. 5845, edited by L. B. Kish, K. Lindenberg, and Z. Gingl (SPIE, Bellingham, WA, 2005), pp. 12–26.

[14] Th. Gallay and G. Raugel, Stability of traveling waves for a damped hyperbolic equation, Z. Angew. Math. Phys. **48**, 451 (1997).

[15] Th. Gallay and G. Raugel, Scaling variables and asymptotic expansions in damped wave equations, J. Diff. Equ. **150**, 42 (1998).

[16] Th. Gallay and G. Raugel, Scaling variables and stability of hyperbolic fronts, SIAM J. Math. Anal. **32**, 1 (2000).

[17] Th. Gallay and G. Raugel, Stability of propagating fronts in damped hyperbolic equations, in *Partial Differential Equations: Theory and Numerical Solutions*, Chapman & Hall Research Notes in Mathematics, Vol. 406, edited by J. Necas, W. Jaeger, J. Stara, O. John, and K. Najzar (Chapman & Hall/CRC Chapman, UK, 2000), pp. 130–146.

[18] K. K. Manne, A. J. Hurd, and V. M. Kenkre, Nonlinear waves in reaction-diffusion systems: The effect of transport memory, Phys. Rev. E **61**, 4177 (2000).

[19] J. M. Sancho and A. Sánchez, Selection, shape, and relaxation fronts: A numerical study of the effects of inertia, Phys. Rev. E **63**, 056608 (2001).

[20] J. A. Gonzalez and F. A. Oliveira, Nucleation theory, the escaping processes, and nonlinear stability, Phys. Rev. B **59**, 6100 (1999).

[21] N. R. Quintero, A. Sánchez, and F. G. Mertens, Anomalous Resonance Phenomena of Solitary Waves with Internal Modes, Phys. Rev. Lett. **84**, 871 (2000).

[22] H. G. Rotstein and A. A. Nepomnyashchy, Dynamics of kinks in two-dimensional hyperbolic models, Physica D **136**, 245 (2000).

[23] J. D. Murray, *Mathematical Biology II: Spatial Models and Biomedical Applications*, 3rd ed., Interdisciplinary Applied Mathematics, Vol. 18 (Springer, New York, 2003).

[24] G. Nicolis and I. Prigogine, *Self-Organization in Nonequilibrium Systems* (Wiley, New York, 1977).

[25] H. Meinhardt, *Models of Biological Pattern Formation* (Academic Press, London, 1982).

[26] P. Borckmans, A. De Wit, and G. Dewel, Competition in ramped Turing structures, Physica A **188**, 137 (1992).

[27] A. De Wit, G. Dewel, P. Borckmans, and D. Walgraef, Three-dimensional dissipative structures in reaction-diffusion systems, Physica D **61**, 289 (1992).

[28] A. J. Koch and H. Meinhardt, Biological pattern formation: From basic mechanisms to complex structures, Rev. Mod. Phys. **66**, 1481 (1994).

[29] D. M. Holloway and L. G. Harrison, Order and localization in reaction-diffusion pattern, Physica A **222**, 210 (1995).

[30] B. Peña and C. Pérez-García, Selection and competition of Turing patterns, Europhys. Lett. **51**, 300 (2000).

[31] L. Yang, A. M. Zhabotinsky, and I. R. Epstein, Stable Squares and other Oscillatory Turing Patterns in a Reaction-Diffusion Model, Phys. Rev. Lett. **92**, 198303 (2004).

[32] D. Iron and J. Rumsey, Stability of asymmetric spike solutions to the Gierer-Meinhardt system, Chaos **17**, 037105 (2007).

[33] A. A. Golovin, B. J. Matkowsky, and V. A. Volpert, Turing pattern formation in the Brusselator model with superdiffusion, SIAM J. Appl. Math. **69**, 251 (2008).

[34] T. Kolokolnikov, J. Wei, and M. Winter, Existence and stability analysis of spiky solutions for the Gierer-Meinhardt system with large reaction rates, Physica D **238**, 1695 (2009).

[35] N. Kumar and W. Horsthemke, Effects of cross diffusion on Turing bifurcations in two-species reaction-transport systems, Phys. Rev. E **83**, 036105 (2011).

[36] E. P. Zemskov, V. K. Vanag, and I. R. Epstein, Amplitude equations for reaction-diffusion systems with cross diffusion, Phys. Rev. E **84**, 036216 (2011).

[37] Y. Nec and M. J. Ward, Dynamics and stability of spike-type solutions to a one dimensional Gierer-Meinhardt model with sub-diffusion, Physica D **241**, 947 (2012).

[38] E. P. Zemskov, K. Kassner, M. J. B. Hauser, and W. Horsthemke, Turing space in reaction-diffusion systems with density-dependent cross diffusion, Phys. Rev. E **87**, 032906 (2013).

[39] G. Gambino, M. C. Lombardo, M. Sammartino, and V. Sciacca, Turing pattern formation in the Brusselator system with nonlinear diffusion, Phys. Rev. E **88**, 042925 (2013).